The Astrophysical Journal, 654:L155–L158, 2007 January 10

NUMERICAL VISCOSITY AND THE SURVIVAL OF GAS GIANT PROTOPLANETS IN DISK SIMULATIONS

Megan K. Pickett[1]
Department of Physics, Lawrence University, Appleton, WI; Megan.Pickett@lawrence.edu
and
Richard H. Durisen
Department of Astronomy, Indiana University, Bloomington, IN
Received 2006 July 20; accepted 2006 November 21; published 2006 December 28

ABSTRACT

We present three-dimensional hydrodynamic simulations of a gravitationally unstable protoplanetary disk model under the condition of local isothermality. Ordinarily, local isothermality precludes the need for an artificial viscosity (AV) scheme to mediate shocks. Without AV, the disk evolves violently, shredding into dense (although short-lived) clumps. When we introduce our AV treatment in the momentum equation, but without heating due to irreversible compression, our grid-based simulations begin to resemble smoothed particle hydrodynamics (SPH) calculations, where clumps are more likely to survive many orbits. In fact, the standard SPH viscosity appears comparable in strength to the AV that leads to clump longevity in our code. This sensitivity to one numerical parameter suggests extreme caution in interpreting simulations by any code in which long-lived gaseous protoplanetary bodies appear.

Subject headings: hydrodynamics — instabilities — planets and satellites: formation — solar system: formation — stars: formation

1. INTRODUCTION

The origin of gas giant planets remains an important issue for understanding the evolution of protoplanetary disks. One formation scenario is the disk instability model. Simulations have shown that massive, cold protoplanetary disks are subject to the rapid appearance of gravitational instabilities (GIs). Although these instabilities have a variety of effects (Durisen et al. 2006), much of the recent interest centers on whether or not GIs lead to gas giant planets (e.g., Boss 1998, 2000, 2001, 2004, 2005; Pickett et al. 1998, 2000, 2003; Mayer et al. 2002, 2004; Rice et al. 2003, 2005; Durisen et al. 2005; Mejía et al. 2005; Cai et al. 2006; Boley et al. 2006). It is clear from simulations that a disk can quickly condense into a complex array of dense features; whether or not anything survives to become a gas giant planet remains an open question. Formation of structure and its long-term maintenance depend on heating and cooling (Pickett et al. 1998, 2000; hereafter collectively PCDL). The survival of a gas giant progenitor is also precarious if a disk is violently unstable. Even dense, compact objects can be destroyed through interaction with the remaining disk, or they may be ejected from the system or accreted onto the star before a single orbit is completed (PCDL; Pickett et al. 2003; Mejía et al. 2005).

Numerical effects may be as critical as physical processes when it comes to fragmentation. For instance, insufficient resolution can act both to prevent (Boss 2001; Pickett et al. 2003) and to trigger (Truelove et al. 1997; Nelson 2003) clump formation. Another crucial effect may be numerical sources of friction and dissipation. The primary tools used for disk simulations have been grid-based codes (e.g., our group and Boss) and smoothed particle hydrodynamics (SPH) codes (e.g., Mayer et al. 2004 and Rice et al. 2003). Of interest to the issue of protoplanet survival is how schemes treat compression as condensations form. For our adiabatic calculations, an artificial viscosity (AV) is needed to treat shocks and satisfy jump conditions, including energy conservation (Pickett et al. 2000). Unmodified AV may be inconsistent under other conditions. Local isothermality, for example, in which temperature is time-independent, precludes a temperature change even in the presence of a strong shock. The resulting internal energy change can be ignored if we assume that heat generated in a shock is radiated away quickly, and AV is then not needed. If included, its dynamical effect would be friction in the momentum equation in compressing flows. Overzealous use of AV could make clumps easier to form and grow. Note, too, that even codes without explicit AV include some analogous friction through their finite accuracy.

Here we present simulations that test the sensitivity of clump survival to the strength of AV in the momentum equation, and we compare these runs as much as possible to the gas physics approximated by SPH. We compute a series of isothermal simulations of a model similar to that in PCDL, in which our AV is implemented with varied strength in the momentum equation but not in the internal energy equation. The motivation for this work is the tendency of SPH simulations to produce protoplanets that survive many orbits (e.g., Mayer et al. 2002, 2004). The concern is that SPH codes require bulk and shear viscosity in order for particles to behave like fluid elements (Monaghan 1992). The longevity of clumps in SPH simulations may in part be an artifact of SPH viscosity.

2. NUMERICAL METHODOLOGY

2.1. *Protostellar Disk Model*

The initial axisymmetric state is made by using a self-consistent field method and a two dimensional hydrodynamics code (Pickett et al. 1998). The resulting equilibrium state contains two distinct regions: a nearly spherical star and a massive, nearly Keplerian disk. The equation of state for the model is that of an $n = 3/2$ polytropic gas: the gas pressure P and the mass density ρ are given by $P = K\rho^{1+1/n}$, with K being a constant. The disk of the model is designed to be unstable, with a Toomre stability parameter $Q \approx 1.35$ and a ratio of disk/star

[1] Also at Department of Chemistry and Physics, Purdue University Calumet, Hammond, IN.

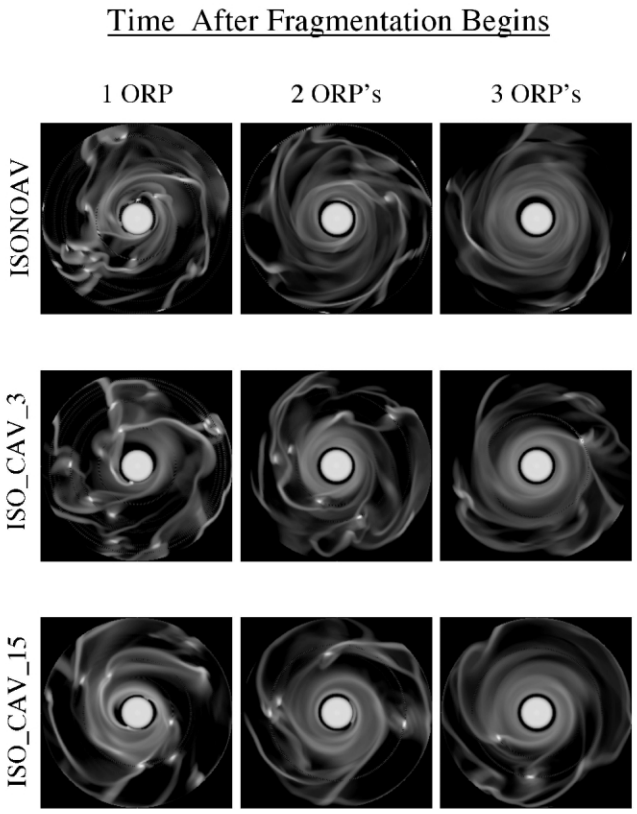

FIG. 1.—Equatorial density gray-scale images for the simulations discussed in this Letter. The gray scale spans 5 orders of magnitude in mass density from black (lowest density) to white (highest density); the same scale is used throughout. Shown are images for the ISO_NOAV case (*top row of panels*), the ISO_CAV_3 case (*middle row of panels*), and the ISO_CAV_15 case (*bottom row of panels*). From left to right, the columns correspond to times equal to 1, 2, and 3 ORPs after fragmentation of the disk begins. Note that the ISO_NOAV disk fragments into many condensations, but this dense substructure has disappeared by the rightmost panel. Although the number of blobs is smaller in the ISO_CAV simulations, they last longer; in each case, a single blob can be traced through three (ISO_CAV_3) and nearly four (ISO_CAV_15) complete orbits before each calculation ends. The original star of the star/disk model is shown in these plots as the white disk in the center.

mass: $M_d/M_s = 0.18$. The model is similar to those studied in PCDL, except that here the star is separated from the disk by a gap and treated as a static point source of gravity (see also Fig. 1).

2.2. *Three-dimensional Hydrodynamics*

The second-order, explicit three-dimensional hydrodynamics code with self-gravity is described in detail in PCDL. The equations of hydrodynamics are solved in conservative fashion on a cylindrical grid with a resolution of $(r, \phi, z) = (128, 512, 16)$. Bulk viscosity is modeled using a von Neumann & Richtmeyer AV scheme (Norman & Winkler 1986). Our AV is designed to account for the real effect of irreversible heating and dissipation that occur in shocks. In locally isothermal simulations, however, inclusion of such heating is not physically consistent, and so we have not used AV in previous isothermal simulations. Thus, the isothermal simulations with AV in this Letter only include AV-induced friction in the momentum equation.

2.3. *Simulation Conditions*

The initially axisymmetric model is loaded into our hydrodynamics grid and given the random cell-to-cell density perturbation $\Delta\rho/\rho = \pm 10^{-3}$ for $r/R_{\rm eq} > 0.5$, where $R_{\rm eq}$ is the initial equatorial radius of the disk. Symmetry about the equatorial plane is assumed, and material is allowed to flow freely off the upper and outer boundaries. Material inside the inner radius $R_{\rm in}$ is not evolved hydrodynamically; instead, the mass interior to $R_{\rm in}$ is treated as a point mass fixed to the center of the grid. Any gas subsequently transported inside $R_{\rm in}$ is added to the central star's mass, and the gravity of the star is included in the disk physics.

TABLE 1
DYNAMICAL TIMES

Simulation	τ_4 (ORP)	P_4 (ORP)	$t_{\rm sat}$ (ORP)	$t_{\rm frag}$ (ORP)	$t_{\rm fin}$ (ORP)
ISO_NOAV	0.11	0.31	0.6	1.4	5.1
ISO_CAV_3	0.15	0.31	0.8	2.3	6.3
ISO_CAV_15	0.20	0.30	1.0	4.0	8.0

We discuss two types of simulations. In the first, denoted ISO_NOAV, the disk is evolved under the locally isothermal condition without AV, as in PCDL. In the second set of simulations, AV is used, but the heating term is not included; these "cold artificial viscosity" (CAV) runs are denoted ISO_CAV. Two long simulations are conducted with different values of the AV coefficient, specifically $C_Q = 3$ and 15 (see eq. [1]). The value of C_Q controls the strength of the AV (Pickett 1995); we have used $C_Q = 3$ in all our published work with AV.

3. RESULTS

Table 1 describes the growth of the dominant nonaxisymmetric mode for the runs; the table lists the growth *e*-folding time for the fastest growing mode (in each case, a four-armed spiral) τ_4, the mode's pattern period P_4, the time at which mode amplitude saturates $t_{\rm sat}$, the time at which the disk begins to fragment $t_{\rm frag}$, and the time each simulation ends $t_{\rm fin}$. All times are measured in outer rotation periods (ORPs). The value of $t_{\rm frag}$ is estimated using images of the midplane to pinpoint the first appearance of a clump: a dense, roughly circular region of gas not connected to another region of similar density. In practice, we look for nonelongated regions of density that correspond to the highest density seen in the spiral arms. Figure 1 shows midplane gray scales of the density at 1, 2, and 2 ORPs after $t_{\rm frag}$. In Table 1 and Figure 1, ISO_CAV_3 and ISO_CAV_15 denote the cases with $C_Q = 3$ and 15, respectively.

The simulations follow a broadly similar evolution, marked by (1) the rapid growth of a four-armed spiral; (2) mode saturation, as measured by a radially averaged Fourier amplitude (Pickett et al. 1998); (3) delayed fragmentation; and (4) evolution of the fragmented disk. During phase 1, as C_Q is increased, the growth rate of the fastest growing mode decreases, but its pattern period remains essentially unaffected. Between saturation and fragmentation, other modes strengthen, and the interaction of these disturbances leads to clump formation.

3.1. *The Locally Isothermal Simulation*

The ISO_NOAV case proceeds in much the same manner as previous locally isothermal simulations of our massive star/disk models (PCDL). Several spirals can be seen in the equatorial images, particularly a two- and four-armed spiral. Although the averaged amplitude of the four-armed disturbance saturates quickly (by 0.6 ORPs), the disk does not fragment until 1 ORP later. The resulting structure is complex and initially includes more than a dozen compact condensations of disk material (see Fig. 1). Table 2 describes the late evolution

TABLE 2
EVOLUTION OF DISK STRUCTURE

Time after Fragmentation	$M_d/M_d(0)$	$J_d/J_d(0)$	N_c	M_c/M_d
ISO_NOAV				
1 ORP	0.53	0.57	15	0.30
2 ORPs	0.33	0.34	1	0.01
3 ORPs	0.26	0.27	0	...
ISO_CAV_3				
1 ORP	0.54	0.60	12	0.30
2 ORPs	0.40	0.41	5	0.20
3 ORPs	0.37	0.36	1	0.08
4 ORPs	0.35	0.34	1	0.09
ISO_CAV_15				
1 ORP	0.69	0.72	7	0.30
2 ORPs	0.47	0.49	4	0.19
3 ORPs	0.37	0.38	2	0.12
4 ORPs	0.34	0.35	1	0.06

of the disk. The table lists the ratio of the disk mass to initial disk mass $M_d/M_d(0)$, the ratio of disk angular momentum to initial disk angular momentum $J_d/J_d(0)$, the number of clumps N_c, and the ratio of the clump mass to disk mass M_c/M_d. Values are reported for fiducial times after fragmentation begins.

The evolution of the ISO_NOAV disk is rapid and violent. One ORP after fragmentation, roughly half the disk mass and angular momentum have been lost. About one-third of the remaining disk mass is contained in 15 clumps. Assuming a solar nebula scaling for the size and mass of the disk, each clump has a mass comparable to Jupiter. Yet, due to the interaction of the remaining disk, none of these potential protoplanets survive an orbit about the central star. Two ORPs after fragmentation, only a single clump remains, and roughly one-third of the disk mass and angular momentum remains on the grid. By the end of the simulation, only one-fourth of the initial disk material is present, and the clumps have disappeared. Roughly 60% of the original disk mass has been accreted by the central regions by the end of the simulations. Despite this vigorous mass transport, we note that the clump disappearance is largely due to disruption *within* the disk.

3.2. *Cold Viscosity Simulations*

In the ISO_CAV_3 simulation, saturation of the fastest growing mode is delayed by 0.2 ORPs, consistent with the slower growth rate, but the time to fragmentation is slowed by an *additional* ORP. Once fragmentation occurs, the evolution of the disk is more quiescent than in the previous case; more of the disk remains 2 ORPs later. Although fewer clumps are initially formed than in ISO_NOAV, later in the run the number and relative mass of clumps are markedly larger (Table 2). Four ORPs after fragmentation, a single clump remains, but it has completed three orbits and contains 10% of the disk mass.

The ISO_CAV_15 simulation of the same protoplanetary disk is even less violent. The time to saturation is now 0.4 ORPs larger than without AV, and more than 3 ORPs are required for fragmentation. Transport in the disk is substantially lower than in the ISO_NOAV case (Table 2) and appears to be asymptoting over the last ORP. Compared to the ISO_CAV_3 simulation, fewer—but higher mass—clumps appear. These condensations survive longer as well; by the end of the simulation, the remaining clump containing 6% of the disk mass has completed nearly five orbits (Fig. 1).

4. DISCUSSION

The stress term in the momentum equation for our AV scheme takes the form of a ram pressure:

$$\mathrm{P}_{\mathrm{AV}}^{\mathrm{grid}} = C_Q \rho (\Delta v)^2, \tag{1}$$

where Δv is the cell-to-cell velocity difference in regions of compression, i.e., where $\Delta v < 0$. AV is zero when $\Delta v > 0$. The value of C_Q is determined empirically (Pickett 1995) by using the Sod shock tube test (Sod 1978).

A number of AV schemes have been used with SPH codes. Typical formulations (e.g., Wadsley et al. 2004) follow Monaghan (1992), in which the bulk AV stress term between two particles is given by

$$\Pi_{\mathrm{ab}} = \beta \mu_{\mathrm{ab}}^2 / \rho_{\mathrm{ab}}. \tag{2}$$

Here, $\beta = 2$, ρ_{ab} is the average density of two SPH particles, and

$$\mu_{\mathrm{ab}} = (h \boldsymbol{v}_{\mathrm{ab}} \cdot \boldsymbol{r}_{\mathrm{ab}}) / [r_{ab}^2 + (\eta h)^2], \tag{3}$$

where $\boldsymbol{v}_{\mathrm{ab}}$ is the difference in relative velocity between the two particles, $\boldsymbol{r}_{\mathrm{ab}}$ is the interparticle distance, and h is the smoothing length. Typically $\eta = 0.1$. The SPH viscosity formulation also has a linear shear term that our formulation does not have. It is also common for SPH simulations of disks to include the Balsara (1995) correction factor to the AV. This AV reduction factor affects only regions dominated by vorticity rather than compression and is ignored here.

To make an approximate comparison between the effects of AV in our grid code simulations and the effects of AV in SPH calculations, we begin by noting that multiplying equation (2) by ρ_{ab}^2 gives it the form of a ram pressure:

$$P_{\mathrm{AV}}^{\mathrm{SPH}} = \beta \rho_{\mathrm{ab}} \mu_{\mathrm{ab}}^2, \tag{4}$$

and therefore

$$P_{\mathrm{AV}}^{\mathrm{SPH}} / P_{\mathrm{AV}}^{\mathrm{grid}} = \beta \rho_{\mathrm{ab}} \mu_{\mathrm{ab}}^2 / C_Q \rho (\Delta v)^2. \tag{5}$$

This ratio represents the relative strength of AV stresses in the momentum equation between the two methodologies.

Turning equation (5) into a quantitative measure depends on how we relate the grid-based Δv to the various SPH variables. Keep in mind that the SPH smoothing length h, like the grid-based cell width Δr, effectively specifies the spatial resolution of a calculation. Let us assume that $\boldsymbol{v}_{\mathrm{ab}} \cdot \boldsymbol{r}_{\mathrm{ab}} / r_{\mathrm{ab}} = f_v \Delta v$, $\rho_{\mathrm{ab}} \approx f_\rho \rho$, and $r_{\mathrm{ab}} = f_h h$, where the f's are, for now, unknown factors. This gives

$$P_{\mathrm{AV}}^{\mathrm{SPH}} / P_{\mathrm{AV}}^{\mathrm{grid}} \approx (\beta / C_Q)(f v^2 f \rho)[1 + (\eta / f_h)^2]^{-1}. \tag{6}$$

Assume, for simplicity, that the density across the smoothing volume is reasonably constant, so $f_\rho \approx 1$. The smoothing length is usually defined so that there are about 50 neighbors within a radius $2h$ from any particle. The typical particle spacing is then roughly $2h/(50)^{1/2} \approx 2h/7$ or $f_h \approx 2/7$. Using $\eta = 0.1$,

$$P_{\mathrm{AV}}^{\mathrm{SPH}} / P_{\mathrm{AV}}^{\mathrm{grid}} \approx 0.89 \beta f v^2 / C_Q. \tag{7}$$

For $f_h \approx \eta$ to 1, the numerical coefficient becomes 0.50 to 0.99, respectively. With the typical values $\beta = 2$ and $C_Q = 3$, the AVs are comparable.

Our analysis suggests that long-lived clumps in SPH simulations of protoplanetary disks may be due, at least in part, to bulk AV, a numerical artifact that is an unavoidable feature of SPH simulations. However, we note that, while AV acts to preserves clumps once formed, if AV is too strong, it may prevent clump formation in the first place. We conducted a further run, in which $C_Q = 21$, and found that the disk did not fragment after nearly 7 ORPs. Althhough we had to stop the calculation due to a numerical problem, the appearance of the disk at the end of the simulation showed no indication of clump formation, consistent with similar tests performed by Mayer et al. (2004). Given the importance of the question and the now demonstrated sensitivity to numerical friction, claims of clump longevity in all codes (e.g., Boss 2000, 2005) should be considered at least somewhat suspect until further analysis, even if an explicit AV is not used.

5. SUMMARY AND CONCLUSIONS

We present simulations of a protoplanetary disk model to study the effects of bulk AV on protoplanetary clump survival. We find that the evolution of the disk is sensitive to the strength of AV; in fact, no clump survives a complete orbit without it. When the viscous effects are strongest, clump longevity is enhanced. Without AV, the disk fragments into many clumps; subsequent collisions can destroy them, shear them into less bound arcs, or significantly alter their orbits. Collisions with AV are demonstrably less violent, since the relative velocity of colliding clumps is reduced.

Our simulations underscore the importance of all aspects of gas physics in the dynamical evolution of protoplanetary disks. This is particularly true when our simulations are compared with SPH methods, which necessarily include a prescription for bulk AV that is as strong as and, under some conditions, perhaps stronger than what is used in our Eulerian code. One issue not directly investigated in these studies is a more direct comparison between the gravitational potential solver resolutions of both methodologies. As a result, it is not entirely clear whether a high enough gravitational resolution simulation with extremely low or nonexistent AV would still produced long-lived clumps. Nevertheless, our simulations sound a strong note of caution when interpreting long-lived clumps seen in any code, unless the numerical friction, whether explicit or implicit, is well understood.

We thank S. Falle, T. Hartquist, J. Monaghan, A. Nelson, and L. Whitehorn-Umphres. We are also indebted to the referee, T. Quinn, whose comments and suggestions greatly improved this manuscript. This work was supported by grant NNG05GN11G from NASA's Origins of Solar Systems Program, grant NAG5-10262 from NASA's Planetary Geology and Geophysics Program, and the Visitor's Program at the University of Leeds.

REFERENCES

Balsara, D. S. 1995, J. Comput. Phys., 121, 357
Boley, A. C., Mejía, A. C., Durisen, R. H., Cai, K., Pickett, M. K., & D'Alessio, P. 2006, ApJ, 651, 517
Boss, A. 1998, ApJ, 503, 923
———. 2000, ApJ, 536, L101
———. 2001, ApJ, 563, 367
———. 2004, ApJ, 610, 456
———. 2005, ApJ, 629, 535
Cai, K., Durisen, R. H., Michael, S., Boley, A. C., Mejía, A. C., Pickett, M. K., & D'Alessio, P. 2006, ApJ, 636, L149
Durisen, R., Boss, A., Mayer, L., Nelson, A., Quinn, T., & Rice, K. 2006, in Protostars and Planets V, ed. B. Reipurth & D. Jewitt (Tucson: Univ. Arizona Press), in press (preprint astro-ph/0603179)
Durisen, R. H., Cai, K., Mejía, A. C., & Pickett, M. K. 2005, Icarus, 173, 417
Mayer, L., Quinn, T., Wadsley, J., & Stadel, J. 2002, Science, 298, 1756
———. 2004, ApJ, 609, 1045
Mejía, A. C., Durisen, R. H., Pickett, M. K., & Cai, K. 2005, ApJ, 619, 1098
Monaghan, J. J. 1992, ARA&A, 30, 543
Nelson, A. F. 2003, in ASP Conf. Ser. 294, Scientific Frontiers in Research on Extrasolar Planets, ed. D. Deming & S. Seager (San Francisco: ASP), 291
Norman, M. L., & Winkler, K.-H. A. 1986, in NATO Advanced Research Workshop on Astrophysical Radiation Hydrodynamics, ed. K.-H. Winkler & M. L. Norman (Dordecht: Reidel), 187
Pickett, B. K. 1995, Ph.D. thesis, Indiana Univ.
Pickett, B. K., Cassen, P., Durisen, R. H., & Link, R. 1998, ApJ, 504, 468
———. 2000, ApJ, 529, 1034
Pickett, B. K., Mejía, A. C., Durisen, R. H., Cassen, P. M., Berry, D. K., & Link, R. P. 2003, ApJ, 590, 1060
Rice, W. K. M., Armitage, P. J., Bate, M. R., & Bonnel, I. A. 2003, MNRAS, 339, 1025
Rice, W. K. M., Lodato, G., & Armitage, P. J. 2005, MNRAS, 364, L56
Sod, G. A. 1978, J. Comput. Phys., 27, 1
Truelove, J. K., Klein, R. I., McKee, C. F., Holliman, J. H., II, Howell, L. H., & Greenough, J. A. 1997, ApJ, 489, L179
Wadsley, J. W., Stadel, J., & Quinn, T. 2004, NewA, 9, 137